MJFAS
Malaysian Journal of Fundamental and Applied Sciences

RESEARCH ARTICLE

Adaptive Bayesian Control Chart for Monitoring Defects in Poisson Process

Yadpirun Supharakonsakun*

Department of Applied Mathematics and Statistics, Faculty of Science and Technology, Phetchabun Rajabhat University, 67000 Phetchabun, Thailand

Abstract This study introduces an enhanced Bayesian c-chart framework by incorporating two novel loss functions: the modified squared error loss function and the K loss function to improve the sensitivity and robustness of process monitoring for attribute data. Unlike traditional control charts that rely on fixed assumptions and static thresholds, the proposed Bayesian approaches dynamically update the control limits by integrating prior information with probabilistic loss structures. The study conducts a comprehensive simulation analysis under various process shift magnitudes and inspection unit sizes and evaluates performance using key indicators, including Average Run Length (ARL), Standard Deviation of Run Length (SDRL), Average Expected Quadratic Loss (AEQL), and the Performance Comparison Index (PCI). The results show that the proposed methods significantly outperform both classical and standard Bayesian c-charts, particularly in detecting small and moderate shifts. Furthermore, applying the proposed control charts to real-world industrial data—specifically defect monitoring in aircraft manufacturing—confirms their practical utility and adaptability. This work contributes a novel perspective to statistical process control (SPC) by integrating flexible Bayesian modeling with customized loss functions and offers a powerful alternative for quality assurance in high-stakes production environments.

Keywords: Bayesian control chart, modified squared error loss function, K loss function, process monitoring, c-chart.

Introduction

Statistical Process Control (SPC) is a foundational methodology for monitoring, controlling, and improving the stability and consistency of manufacturing and service processes. It uses statistical tools, most notably control charts, to detect deviations from normal process behavior [1] and enables early intervention to prevent defective outputs and maintain product quality [2,3]. Among the various control charts in SPC, the c-chart is particularly suitable for tracking discrete count-type data, such as the number of defects or nonconformities per inspection unit over time [4–5]. This chart is especially applicable when the occurrence of nonconformities follows the Poisson distribution, which models rare and independent events occurring within fixed intervals of time, space, or product volume.

In quality control contexts, a nonconforming item refers to a product unit that fails to meet one or more specified requirements. Each individual violation of a requirement is termed a defect or nonconformity. A single unit may contain multiple nonconformities and still be classified as nonconforming, depending on the nature and severity of those defects. Although the Poisson distribution provides a sound theoretical foundation for modeling such data, real-world processes do not always satisfy its assumptions, such as having constant defect probability or infinite opportunities for defects. However, when these deviations are minor, the Poisson model remains a practical approximation. In contrast, severe violations of these assumptions can diminish the model's reliability, highlighting the need for more adaptive control strategies.

To construct a traditional c-chart, practitioners compute the average number of nonconformities, often denoted as, from the observed data. This average forms the basis for establishing the control limits. Under the assumption that the defect count follows a Poisson distribution, the control limits for the c-chart are calculated as follows:

***For correspondence:**
yadpirun.suph@pcru.ac.th

Received: 4 August 2025
Accepted: 5 Jan. 2026

$$\begin{aligned} UCL &= \mu + 3\sqrt{\mu}, \\ CL &= \mu, \\ LCL &= \mu - 3\sqrt{\mu}, \end{aligned} \quad (1)$$

in which CL denotes the center line, and UCL and LCL represent the upper and lower control limits, respectively [6]. If the resulting lower control limit (LCL) is negative, it is conventionally set to zero, as negative defect counts are not meaningful.

Although the classical (frequentist) approach to constructing c-charts is well-established and widely adopted, it often lacks the adaptability required in dynamic or uncertain environments, particularly when detecting small to moderate process shifts [7,8]. In response to these limitations, Bayesian methods have attracted increasing interest due to their ability to incorporate prior knowledge and update inferences as new data become available. Numerous studies demonstrate the superiority of Bayesian methods over classical statistical approaches in SPC, particularly in terms of decision-making during out-of-control states, optimal sample sizes, and update frequency—enabled by posterior probability [9–11]. Research has explored a variety of Bayesian applications in SPC, such as constructing control charts for the process mean and variance under the assumption of a normal distribution [12–14], improving Bayesian Exponentially Weighted Moving Average (EWMA) charts [15], and modifying EWMA charts based on normality assumptions [16]. Additionally, Bayesian updating schemes have been developed for Shewhart, CUSUM, and EWMA control charts with normally distributed observations [17]. A Bayesian EWMA control chart based on the inverse Gaussian process was also introduced to improve change detection performance [18–19]. Beyond the normal distribution, Bayesian methods have been effectively applied to processes governed by other distributions, such as the exponential distribution [20].

Significant Bayesian advancements have also been made for control charts based on the Poisson distribution. For instance, Assareh *et al*. [21] proposed a Bayesian hierarchical model to estimate change points in Poisson processes, which was integrated into control schemes including the c-chart, EWMA, and CUSUM charts. This approach has been used to establish control limits for nonconformities [7, 23–24], with results consistently outperforming classical methods.

A critical aspect of Bayesian inference lies in the choice of the loss function, which defines how the model penalizes estimation errors. Mitchell *et al*. [25] developed a Bayesian EWMA chart for Poisson processes using several loss functions—including squared error, LINEX, and entropy—demonstrating notable improvements. Other studies introduced Bayesian c-charts incorporating priors such as Jeffreys' prior [23] and the gamma prior [7], reporting better Average Run Length (ARL) and false alarm rates compared to frequentist alternatives. More recently, an empirical Bayes approach using an exponential prior has further enhanced c-chart performance [24]. Collectively, these studies reinforce the effectiveness of Bayesian methods in improving SPC utility.

While the squared error loss function is commonly used, it may not adequately reflect asymmetric risk preferences or the practical cost structures encountered in industrial settings. The modified squared error and K loss functions have shown superior performance, achieving lower ARL1 and greater sensitivity in detecting parameter shifts in inverse Gaussian processes [18–19].

To address these challenges, this study proposes and evaluates two alternative loss functions—the modified squared error loss and the K loss function—within a Bayesian framework, aiming to improve the sensitivity and adaptability of c-charts for detecting subtle shifts in Poisson-distributed processes. These loss functions are designed to enhance detection performance while maintaining robustness across varying sample sizes and shift magnitudes. By integrating these loss functions into the Bayesian estimation process, the proposed method allows for more accurate and responsive determination of control limits for count data.

The proposed approach is validated through simulation studies and real-world applications, using performance metrics such as Average Run Length (ARL), Standard Deviation of Run Length (SDRL), Average Extra Quadratic Loss (AEQL), and the Performance Comparison Index (PCI). Although researchers commonly use ARL to evaluate detection speed, ARL values often vary across different shift sizes, which may lead to inconclusive performance comparisons when ARL is considered alone. Therefore, this study employs AEQL and PCI to provide a more comprehensive evaluation of overall detection efficiency across a range of shift magnitudes. Results indicate that Bayesian c-charts developed under the modified squared error and K loss functions exhibit superior performance—particularly in identifying small to moderate process shifts—thereby offering more effective and practical tools for quality monitoring in modern industrial environments.

Bayesian Inference in Quality Control

The c-chart, or count chart, is specifically designed for monitoring processes that involve discrete and countable events. It is particularly well-suited for tracking the number of defects per unit, batch, or defined inspection area over time. This type of control chart operates under the assumption that the number of nonconformities follows a Poisson distribution, which is appropriate for modeling rare, independent events that occur over a fixed interval of time or space.

In constructing a c-chart, it is assumed that the number of nonconformities observed during each inspection follows a Poisson distribution with a specified mean parameter μ . When inspections are conducted at regular intervals, the count of nonconformities in the i^th^ sample is modeled accordingly, as described by the following formulation:

$$f\left(x_i \mid \mu\right)=\frac{\mu^{x_i} e^{-\mu}}{x_i!},\; x_i=0,1,2,\ldots;\; i=1,\ldots,m: \mu>0. \tag{2}$$

To apply the Bayesian methodology for estimating the mean parameter μ of a Poisson distribution, this study adopts a conjugate prior, specifically the Gamma distribution, due to its analytical convenience and mathematical compatibility with the Poisson likelihood. Following the approaches outlined by Supharakonsakun [7] and Song & Kim [26], the prior distribution for μ is defined as:

$$\mu \sim Gamma(a,b) \tag{3}$$

where *a* and *b* are the shape and rate parameters of the Gamma distribution, respectively. This choice ensures that the posterior distribution also belongs to the Gamma family, facilitating closed-form updates and interpretations.

By applying Bayes' theorem, the posterior distribution of μ is obtained through the product of the likelihood function (derived from the observed Poisson data) and the prior distribution:

$$g\left(\mu \mid X\right) \propto L\left(x \mid \mu\right)\pi\left(\mu\right). \tag{4}$$

Substituting the expressions for the Poisson likelihood and Gamma prior yields the posterior distribution, which also follows a Gamma form with updated parameters:

$$\mu \mid X \sim Gamma\left(a+\sum_{i=1}^{m} x_i, b+m\right). \tag{5}$$

Here, $\sum_{i=1}^{m} x_i$ is the total number of observed nonconformities over *m* inspection units. These updated hyper-parameters reflect the integration of both prior beliefs and empirical data within the Bayesian framework, allowing for adaptive inference that evolves with additional information.

A key feature of Bayesian estimation lies in the incorporation of loss functions, which serve as formal mechanisms for quantifying the consequences of estimation errors. Loss functions guide decision-making by linking statistical inference to the real-world costs or risks associated with incorrect estimates. Formally, a loss function $L(\mu,\hat{\mu})$ expresses the penalty for estimating a parameter μ by $\hat{\mu}$, and the Bayesian risk, the expected loss with respect to the posterior distribution, serves as the criterion for selecting an optimal estimator.

The concept of loss functions in Bayesian decision theory was introduced by Wald [27], and has since become foundational in the development of robust statistical estimators. Various types of loss functions have been proposed to reflect different estimation priorities or application-specific considerations, as demonstrated in [28].

In the context of this study, Bayesian estimation of the Poisson mean is enhanced through the use of two alternative loss functions: the modified squared error loss and the K loss function. These formulations offer increased sensitivity and robustness compared to the traditional squared error loss, particularly in the setting of quality control where asymmetric costs or subtle process changes are relevant. By incorporating these advanced loss functions, the Bayesian c-chart becomes more effective in detecting small to moderate shifts, making it a powerful tool for industrial process monitoring and quality assurance.

Bayesian Estimation under Modified Squared Error Loss Function

The modified squared error loss function (MSELF) represents a refined alternative to the traditional squared error loss function (SELF), specifically designed to accommodate asymmetry and contextual sensitivity in estimation tasks. While the classical SELF, defined as $L(\mu,\hat{\mu})=(\mu-\hat{\mu})^2$, is popular for its mathematical convenience and widespread application in regression, machine learning, and control chart analysis, it assumes symmetrical penalization of estimation errors. This assumption may not hold in many quality control contexts, where underestimation and overestimation could have unequal consequences.

To understand the motivation for modifying this classical form, it is first important to examine how the Bayesian estimator operates under the original squared error loss function. The Bayesian estimator under the squared error loss function (SELF) is obtained by minimizing the posterior risk, which corresponds to the expected value of the posterior distribution. This yields the well-established form:

$$\hat{\mu}_{SELF}=E\left(\mu\mid X\right)=\frac{a+\sum_{i=1}^{m}x_i}{b+m}. \tag{6}$$

In contrast, the Modified Squared Error Loss Function (MSELF) modifies this framework by introducing asymmetry in the penalization of prediction errors, thereby addressing a critical limitation of the traditional SELF. In many real-world quality control scenarios, the consequences of underestimating a defect rate can differ significantly from overestimating it—for example, underestimation might lead to undetected process deterioration, whereas overestimation may trigger unnecessary interventions. MSELF accounts for this imbalance by altering the loss structure to weigh errors differently depending on their direction.

As proposed by [29], the MSELF is defined as:

$$L(\mu,\hat{\mu})=\left(1-\frac{\hat{\mu}}{\mu}\right)^2. \tag{7}$$

This non-symmetric formulation penalizes relative deviation rather than absolute squared differences, making it more suitable for skewed cost structures or contexts where proportional accuracy is essential. The corresponding Bayesian estimator under MSELF minimizes the posterior risk with respect to this adjusted loss and is expressed as:

$$\hat{\mu}_{MSELF}=\frac{E\left(\mu^{-1}\mid X\right)}{E\left(\mu^{-2}\mid X\right)}. \tag{8}$$

This form yields a Bayesian estimator that adapts to both the structure of the data and the asymmetric costs associated with estimation errors, thereby enhancing the performance of control charts in detecting shifts in Poisson-based processes, particularly in the context of the c-chart. Based on the posterior distribution derived in Equation (5), the Bayesian estimator under the entropy loss function [30] is obtained from the posterior density of the reciprocal of μ and is expressed as:

$$E\left(\mu^{-1}\mid X\right)=\frac{b+m}{a-1+\sum_{i=1}^{m}x_i}. \tag{9}$$

Additionally, consider

$$E\left(\mu^{-2}\mid X\right)=\int_0^\infty \mu^{-2}\frac{\left(b+m\right)^{a+\sum_{i=1}^{m}x_i}e^{-\mu(b+m)}\mu^{a+\sum_{i=1}^{m}x_i-1}}{\Gamma\left(a+\sum_{i=1}^{m}x_i\right)}d\mu$$
$$=\frac{\left(b+m\right)^2}{\left(a-1+\sum_{i=1}^{m}x_i\right)\left(a-2+\sum_{i=1}^{m}x_i\right)}.$$

Therefore, the Bayesian estimator of the parameter μ under MSELF is given by:

The MSELF-based estimator effectively addresses the limitations of symmetric loss functions by incorporating asymmetry into the estimation process, enhancing the chart's responsiveness to small shifts. The following section presents the K loss function, an alternative asymmetric approach designed to further improve Bayesian estimation in Poisson-based quality control.

Bayesian Estimation under K Loss Function

The K loss function (KLF) serves as an alternative loss function frequently employed in fields such as machine learning and statistical optimization. By minimizing this loss function, practitioners can effectively estimate model parameters or improve model performance through various optimization techniques. Its structure is particularly suited to scenarios where asymmetry in error penalization is desired, thereby contributing to enhanced model accuracy and robustness. The KLF has been applied in prior studies (cf. [31, 32]) and is mathematically defined as:

$$L(\mu,\hat{\mu}) = \left(\sqrt{\frac{\mu}{\hat{\mu}}} - \sqrt{\frac{\hat{\mu}}{\mu}}\right)^2. \quad (11)$$

Under this loss framework, the Bayesian estimator (BE) is expressed as:

$$\hat{\mu}_{KLF} = \sqrt{\frac{E(\mu \mid X)}{E(\mu^{-1} \mid X)}}. \quad (12)$$

where $E(\mu \mid X)$, the expected value of the posterior distribution, is provided by equation 6, $E(\mu^{-1} \mid X)$ is defiened by equation 9. This formulation reflects a balance between inverse and direct expectations, enhancing the sensitivity and adaptability of parameter estimation for Poisson-distributed processes. Based on the estimated parameter μ, the control limits for the c-chart are then constructed as follows:

$$\hat{\mu}_{KLF} = \frac{\sqrt{\left(a-1+\sum_{i=1}^{m} x_i\right)\left(a+\sum_{i=1}^{m} x_i\right)}}{b+m}. \quad (13)$$

The two proposed estimators, namely MSELF and KLF, derived using the Bayesian approach, are employed to construct the control limits of the c-chart based on the parameter μ. These estimators are also compared with the traditional SELF estimator [33] and the classical c-chart method. The results of this comparative study, based on simulation experiments, are presented in the following section.

Experimental Results

The study performs simulation experiments using the R programming language to assess the performance of the three methods across a range of shift sizes: 0.1, 0.5, 1.0, 2.0, 3.0, 5.0, 10.0, 20.0, and 30.0. The in-control average run length (ARL_0) was fixed at 370.

Table 1 summarizes the ARL and SDRL values obtained from both classical and Bayesian methods for inspection unit sizes of 20, 40, and 100 using hyper-parameters $(\nu,\gamma)=(3,1)$. The Bayesian method employing the modified squared error loss function consistently yields lower ARL_1 and $SDRL_1$ values across all shift magnitudes for $m=20$ and $m=100$, except at shift sizes of 0.1 and 0.5 for $m=40$, where the Bayesian method under the K loss function performs better. Additionally, the AEQL and PCI values reinforce the superior performance of the Bayesian method with the modified squared error loss function, as it achieves the lowest AEQL and a PCI of 1, indicating high effectiveness in detecting process shifts.

Table 1. Comparison of ARL and SDRL Values for Various Methods at $(\nu,\gamma)=(3,1)$

m	δ	Classical		SE_LF		MSE_LF		K_LF	
		ARL	SDRL	ARL	SDRL	ARL	SDRL	ARL	SDRL
20		L=3.030		L=3.186		L=3.209		L=3.192	
	0.0	370.7735	370.2732	370.0493	369.5490	369.2469	368.7466	371.0255	370.5252
	0.1	354.0583	353.5580	354.0583	347.1513	346.2918	345.7915	348.3431	347.8428
	0.5	292.4151	291.9147	269.1632	268.6627	267.0885	266.5880	269.4933	268.9928
	1.0	222.7292	192.9444	192.8214	192.3207	190.5848	190.0841	192.9444	192.4438
	2.0	123.1672	122.6662	101.2406	100.7393	99.8400	99.33875	101.2509	100.7497
	3.0	67.9865	67.4846	55.5578	55.0555	54.8147	54.3124	55.5567	55.0544
	5.0	24.2166	23.7113	20.3877	19.8814	20.1379	19.6314	20.3863	19.8800
	10.0	4.2531	3.71959	3.8481	3.3106	3.8223	3.2844	3.8479	3.3103
	15.0	1.7545	1.15053	1.6684	1.0560	1.6628	1.0499	1.6683	1.0559
	20.0	1.1954	0.48323	1.1954	0.4479	1.1696	0.4455	1.1713	0.4479
	30.0	1.0085	0.09254	1.0070	0.0839	1.0069	0.0833	1.0070	0.0839
AEQL		383.2017		347.5444		344.3063		346.6773	
PCI		1.1130		1.0094		1.0000		1.0069	
40		L=3.0331		L=3.118		L=3.13		L=3.12	
	0.0	369.6355	369.1352	371.1875	370.6872	370.6425	370.1421	370.6425	370.9983
	0.1	348.1529	347.6525	346.8551	346.3547	346.0280	345.5276	347.0980	346.5977
	0.5	276.5531	276.0527	267.3952	266.8947	266.0422	265.5417	267.4646	266.9642
	1.0	203.9975	203.4969	192.232	191.7313	191.1067	190.6061	192.1695	191.6689
	2.0	109.2953	108.7942	101.1262	100.625	100.4756	99.9744	101.0657	100.5644
	3.0	60.7265	60.2245	56.2093	55.7071	55.8259	55.3236	56.1841	55.6819
	5.0	22.2697	21.7639	20.8446	20.3384	20.7331	20.2270	20.8383	20.3322
	10.0	4.0999	3.5650	3.9426	3.4061	3.9299	3.3933	3.9421	3.4056
	15.0	1.7279	1.1214	1.6946	1.0850	1.6921	1.0823	1.6945	1.0849
	20.0	1.1884	0.4731	1.1788	0.4592	1.1781	0.4581	1.1788	0.4591
	30.0	1.0078	0.0888	1.0072	0.0854	1.0072	0.0851	1.0072	0.0854
AEQL		363.4752		349.7816		348.6521		349.7142	
PCI		1.0425		1.0032		1.0000		1.0030	
100		L=3.036		L=3.077		L=3.0802		L=3.0778	
	0.0	370.6344	370.1341	372.0322	371.5319	370.053	369.5526	369.5554	369.0551
	0.1	349.7837	349.2833	349.597	349.0967	347.7073	347.2069	347.3597	346.8593
	0.5	270.9747	270.4742	268.5872	268.0868	266.9847	266.4842	266.8603	266.4842
	1.0	196.0822	195.5815	193.3464	192.8457	192.1461	191.6455	192.1649	191.6643
	2.0	104.0534	103.5522	102.2407	101.7395	101.5912	101.0900	101.6258	101.1246
	3.0	58.18679	57.6846	57.14574	56.64353	56.78713	56.2849	56.81623	56.3140
	5.0	21.4780	20.9720	21.1467	20.6407	21.0397	20.53368	21.0474	20.5413
	10.0	4.0439	3.5084	4.0074	3.4715	3.9962	3.4602	3.9967	3.4608
	15.0	1.7215	1.1145	1.7135	1.1057	1.7109	1.1029	1.71114	1.1031
	20.0	1.1856	0.4691	1.1832	0.4656	1.1825	0.4645	1.1825	0.4646
	30.0	1.0075	0.0873	1.0074	0.0866	1.0074	0.0863	1.0074	0.0863
AEQL		356.0805		352.9226		351.8221		351.8840	
PCI		1.0121		1.0031		1.0000		1.0002	

Table 2 presents results for hyper-parameters $(\nu,\gamma)=(3,2)$. The Bayesian method under the modified squared error loss function again demonstrates consistent superiority in terms of ARL_1 and $SDRL_1$ for all shift magnitudes when $m=20$ and $m=100$. However, at a shift size of 0.1 for $m=40$, the K loss function produces lower ARL_1 and $SDRL_1$. The AEQL and PCI metrics confirm the effectiveness of the modified squared error loss function, delivering the lowest AEQL and a PCI of 1.

Table 2. Comparison of ARL and SDRL Values for Various Methods at $(\nu,\gamma)=(5,1)$

m	δ	Classical		SE_LF		MSE_LF		K_LF	
		ARL	SDRL	ARL	SDRL	ARL	SDRL	ARL	SDRL
20		*L*=3.0300		*L*=3.1638		*L*=3.1850		*L*=3.1674	
	0.0	370.2394	369.7391	370.3544	369.7391	369.3033	368.803	369.5702	369.0698
	0.1	356.9660	356.4656	351.1353	350.6349	349.2805	348.7801	350.0496	349.5492
	0.5	292.8414	292.3409	271.3079	270.8075	269.0716	268.5711	270.1945	269.6941
	1.0	220.7979	220.2973	193.7088	193.2082	191.2284	190.7278	192.7712	192.2706
	2.0	122.5810	122.0800	102.4111	101.9099	100.8911	100.3899	101.7987	101.2974
	3.0	68.0761	67.5742	56.5655	56.0633	55.7409	55.2387	56.2583	55.7560
	5.0	24.1691	23.6638	20.5918	20.0856	20.3271	19.8208	20.4864	19.9801
	10.0	4.2461	3.7125	3.8700	3.3327	3.8411	3.3035	3.8591	3.3216
	15.0	1.7569	1.1531	1.6780	1.0666	1.6715	1.05953	1.6755	1.0638
	20.0	1.1953	0.4831	1.1730	0.4505	1.1711	0.4476	1.1723	0.4494
	30.0	1.0084	0.0923	1.0070	.08438	1.0069	0.0837	1.0070	0.0841
AEQL		382.7643		348.9660		346.3861		347.9652	
PCI		1.1050		1.0074		1.0000		1.0046	
40		*L*=3.033267		*L*=3.105702		*L*=3.1178		*L*=3.1086	
	0.0	369.1496	368.6493	371.1234	370.623	370.1452	369.6449	369.7327	369.2324
	0.1	349.5763	349.0759	349.1722	348.6718	347.7231	347.2227	347.676	347.1756
	0.5	277.3475	276.8471	269.4819	268.9815	267.905	267.4046	268.2798	267.7793
	1.0	204.6179	204.1173	193.849	193.3483	192.4279	191.9272	193.065	192.5644
	2.0	109.6025	109.1014	102.241	101.7398	101.3596	100.8583	101.7760	101.2747
	3.0	61.1300	60.6279	56.9587	56.4564	56.4945	55.9922	56.7322	56.2300
	5.0	22.1610	21.6552	20.9000	20.3939	20.7520	20.2458	20.8232	20.3170
	10.0	4.0980	3.5631	3.9626	3.4263	3.9456	3.4092	3.9531	3.4167
	15.0	1.7308	1.1247	1.7005	1.1247	1.6968	1.0874	1.6983	1.0890
	20.0	1.1876	0.4721	1.1792	0.4596	1.1781	0.4581	1.1786	0.4588
	30.0	1.0078	0.0887	1.0072	0.0857	1.0072	0.0854	1.0072	0.0855
AEQL		363.7587		351.4396		349.9664		350.6575	
PCI		1.0394		1.0042		1.0000		1.0020	
100		*L*=3.035		*L*=3.072		*L*=3.0769		*L*=3.0732	
	0.0	369.8346	369.3343	370.1652	369.6649	370.0078	369.5075	370.4187	369.9183
	0.1	347.2094	346.7091	347.1094	346.609	346.7774	346.2770	347.3818	346.8814
	0.5	271.3177	270.8172	269.303	268.8026	268.8139	268.3134	269.4189	268.9185
	1.0	195.6439	195.1433	193.1434	192.6427	192.5623	192.0616	193.1849	192.6843
	2.0	103.6814	103.1802	102.0019	101.5006	101.6254	101.1242	102.0066	101.5053
	3.0	57.9101	57.40795	56.95117	56.4489	56.7491	56.2468	56.95202	56.4498
	5.0	21.4002	20.8942	21.1150	20.6090	21.04915	20.5430	21.1150	20.6090
	10.0	4.0409	3.5054	4.0081	3.4723	4.0015	3.4656	4.0081	3.4723
	15.0	1.7200	1.1129	1.7133	1.1054	1.7117	1.10381	1.7133	1.1054
	20.0	1.1856	0.4691	1.1836	0.4662	1.1832	0.4655	1.1836	0.4662
	30.0	1.0075	0.0872	1.0074	0.0865	1.0074	0.0863	1.00743	0.0865
AEQL		355.4497		352.6169		351.9935		352.6284	
PCI		1.0098		1.0018		1.0000		1.0018	

Table 3 displays outcomes for hyper-parameters $(\nu,\gamma)=(2,2)$. For $m=20$, the original squared error loss function performs better for shift sizes ranging from 0.1 to 2.0, while the modified squared error loss function shows superior performance for larger shift sizes (3.0–30). For $m=40$, the original squared error loss function yields better results for shift sizes 0.1 to 5.0. Beyond that, all three Bayesian loss functions offer comparable and improved ARL_1 and $SDRL_1$ values. When $m=100$, the modified squared error loss function consistently outperforms others across all shift magnitudes. Furthermore, AEQL and PCI values confirm the advantage of the original squared error loss function for $m = 20$ and $m = 40$, whereas the modified squared error loss function provides the best performance for $m = 100$, as indicated by the lowest AEQL and PCI of 1.

Table 3. Comparison of ARL and SDRL Values for Various Methods at $(\nu, \gamma) = (2,2)$

m	δ	Classical ARL	Classical SDRL	SE_LF ARL	SE_LF SDRL	MSE_LF ARL	MSE_LF SDRL	K_LF ARL	K_LF SDRL
20		*L*=3.028		*L*=3.44123		*L*=3.4672		*L*=3.4461	
	0.0	369.849	369.3486	369.1893	368.689	370.6262	370.1258	369.6967	369.1964
	0.1	354.0463	353.5459	346.3065	345.8061	347.4936	346.9932	346.7114	346.2111
	0.5	291.4196	290.9192	255.5689	255.0685	256.0021	255.5016	255.7305	255.2301
	1.0	219.5311	219.0305	177.5188	177.0181	177.6708	177.1701	177.5797	177.0790
	2.0	121.8304	121.3294	92.5576	92.0563	92.5614	92.0600	92.5629	92.0615
	3.0	67.4088	66.9069	51.0472	50.5447	51.0429	50.5404	51.0477	50.5452
	5.0	24.1603	23.6550	19.0057	18.4990	19.0033	18.4965	19.0057	18.4990
	10.0	4.24324	3.7097	3.6946	3.1552	3.6941	3.1548	3.6946	3.1552
	15.0	1.7551	1.1512	1.6380	1.0223	1.6379	1.0222	1.6380	1.0223
	20.0	1.1951	0.4829	1.1621	0.4340	1.1620	0.4339	1.1621	0.4340
	30.0	1.0084	0.0924	1.0064	0.0806	1.0064	0.0806	1.0064	0.0806
AEQL		381.7051		332.5711		332.5780		332.5830	
PCI		1.1477		1.0000		1.0000		1.0000	
40		*L*=3.0332		*L*=3.24		*L*=3.2542		*L*=3.2445	
	0.0	370.2352	369.7349	370.5896	370.0893	371.7887	371.2884	370.9207	370.4204
	0.1	349.1937	348.6933	343.6186	343.1182	344.6628	344.1624	343.8839	343.3835
	0.5	277.819	277.3185	258.8706	258.3701	259.284	258.7835	258.9866	258.4861
	1.0	204.1933	203.6927	183.3099	182.8092	183.4671	182.9664	183.3495	182.8488
	2.0	109.5819	109.0807	95.5600	95.0587	95.5791	95.07781	95.5648	95.0634
	3.0	60.9648	60.4628	53.2218	52.7194	53.2242	52.7218	53.2225	52.7201
	5.0	22.2162	21.7104	19.7996	19.2931	19.7997	19.2932	19.7996	19.2931
	10.0	4.1005	3.5656	3.8342	3.2965	3.8342	3.2965	3.8342	3.2965
	15.0	1.7298	1.1235	1.6720	1.06005	1.6720	1.0600	1.6720	1.0600
	20.0	1.1881	0.4728	1.1717	0.4486	1.1717	0.4486	1.1717	0.4486
	30.0	1.0078	0.0887	1.0068	0.0829	1.0068	0.0829	1.0068	0.0829
AEQL		363.7337		340.1918		340.2256		340.2006	
PCI		1.0692		1.0000		1.0001		1.0000	
100		*L*=3.035		*L*=3.1258		*L*=3.13028		*L*=3.1273	
	0.0	370.2295	369.7292	369.9150	369.4146	369.3215	368.8212	370.2083	369.7079
	0.1	348.7439	348.2435	346.0318	345.5314	345.4383	344.9380	346.2731	345.7728
	0.5	270.2833	269.7828	263.341	262.8405	262.6128	262.1124	263.4483	262.9478
	1.0	195.4063	194.9056	187.8414	187.3408	187.2047	186.7041	187.8783	187.3777
	2.0	103.9161	103.4149	99.1849	98.6837	98.8594	98.3581	99.19025	98.6889
	3.0	57.9538	57.4516	55.3578	54.8555	55.1713	54.6690	55.3586	54.8563
	5.0	21.4423	20.9364	20.6459	20.1397	20.5879	20.0816	20.6459	20.1397
	10.0	4.0436	3.5082	3.9523	3.4159	3.9460	3.4095	3.9523	3.4159
	15.0	1.7209	1.1139	1.7008	1.0918	1.6994	1.0902	1.7008	1.0918
	20.0	1.1856	0.46923	1.1799	0.4608	1.1795	0.4602	1.1799	0.4608
	30.0	1.0075	0.0871	1.0072	0.0851	1.0071	0.0850	1.0072	0.0851
AEQL		355.6657		347.6904		347.1040		347.6990	
PCI		1.0247		1.0017		1.0000		1.0017	

Table 4. Comparison of ARL and SDRL Values for Various Methods at $(\nu,\gamma)=(1,2)$

m	δ	**Classical**		**SE_LF**		**MSE_LF**		**K_LF**	
		ARL	**SDRL**	**ARL**	**SDRL**	**ARL**	**SDRL**	**ARL**	**SDRL**
		L=3.0303		L=3.452956		L=3.48271		L=3.460904	
	0.0	370.7821	370.2818	369.7474	369.2470	370.7976	370.2973	370.1375	369.6372
	0.1	354.4800	353.9796	341.0916	340.5912	341.9072	341.4068	341.4472	340.9469
	0.5	292.2754	291.775	255.6170	255.1165	255.9237	255.4232	255.7339	255.2334
	1.0	220.9209	220.4203	178.4737	177.973	178.5629	178.0622	178.5158	178.0151
20	2.0	122.4405	121.9395	92.2928	91.7914	92.2912	91.7898	92.2967	91.7953
	3.0	68.0922	67.5903	51.3517	50.8493	51.3471	50.8447	51.3522	50.8498
	5.0	24.0404	23.5351	18.8545	18.3477	18.8519	18.3451	18.8545	18.3477
	10.0	4.2418	3.7083	3.6896	3.1502	3.6892	3.1498	3.6896	3.1502
	15.0	1.7572	1.1535	1.6388	1.0232	1.6387	1.0231	1.6388	1.0232
	20.0	1.1953	0.4832	1.1622	0.4341	1.1621	0.4341	1.1621	0.4341
	30.0	1.0084	0.0924	1.0064	0.0805	1.0064	0.0805	1.0064	0.0805
AEQL		382.3969		332.4380		332.4342		332.4430	
PCI		1.1503		1.0000		1.0000		1.0000	
		L=3.033274		L=3.249328		L=3.2625		L=3.2528	
	0.0	369.0625	368.5622	371.1777	370.6773	370.0912	369.5909	369.4311	368.9308
	0.1	350.4509	349.9505	345.9368	345.4365	344.7692	344.2689	344.2758	343.7754
	0.5	277.9077	277.4072	259.7607	259.2602	258.5613	258.0609	258.3443	257.8438
	1.0	278.4781	277.9776	260.5958	260.0953	259.4468	258.9463	259.2254	258.7249
	2.0	204.4007	203.9001	183.2342	182.7335	182.3863	181.8857	182.3062	181.8055
40	3.0	110.1477	109.6466	96.04773	95.54643	95.5546	95.0532	95.5441	95.0427
	5.0	61.2814	60.7794	53.4716	52.9693	53.2230	52.7207	53.2215	52.7191
	10.0	22.2349	21.7291	19.8470	19.3406	19.7673	19.2608	19.7672	19.2607
	15.0	4.0998	3.5649	3.8353	3.2976	3.8254	3.2876	3.8254	3.2876
	20.0	1.1883	0.4730	1.1722	0.4494	1.1716	0.4484	1.1716	0.4484
	30.0	1.0078	0.0890	1.0069	0.0833	1.0068	0.0831	1.0068	0.0831
AEQL		747.3374		680.5349		678.1683		678.1008	
PCI		1.1021		1.0036		1.0001		1.0000	
		L=3.035		L=3.129		L=3.133		L=3.13	
	0.0	370.6839	370.1836	370.3589	369.8586	370.1332	369.6329	370.6419	370.1415
	0.1	349.5591	349.058	346.9394	346.4391	346.5509	346.0505	347.1779	346.6776
	0.5	270.0386	269.5382	262.9620	262.4615	262.3382	261.8377	263.0578	262.5574
	1.0	195.5550	195.0544	188.2198	187.7192	187.6284	187.1278	188.2526	187.7519
	2.0	104.1500	103.6488	99.3814	98.8801	99.04721	98.5459	99.38596	98.8847
100	3.0	58.0599	57.5577	55.5251	55.0228	55.3622	54.8599	55.5258	55.0235
	5.0	21.4661	20.9601	20.6520	20.1458	20.5957	20.0895	20.6520	20.1458
	10.0	4.0386	3.5030	3.9464	3.4100	3.9403	3.4037	3.9464	3.4100
	15.0	1.7208	1.1137	1.7009	1.0918	1.6995	1.0904	1.7009	1.0918
	20.0	1.1857	0.4693	1.1800	0.4609	1.1797	0.4604	1.1800	0.4609
	30.0	1.0075	0.0872	1.0072	0.0853	1.0072	0.0851	1.0072	0.0853
AEQL		355.8565		347.8912		347.3452		347.8989	
PCI		1.0245		1.0016		1.0000		1.0016	

Table 4 presents results for hyper-parameters $(\nu,\gamma)=(1,2)$. For $m=20$, the original squared error loss function performs better at detecting small shifts (0.1–1.0), while the modified squared error loss function excels for larger shifts (2.0–30). For $m=40$, the K loss function offers better detection at shift sizes 0.1 to 10.0, whereas both the original and modified squared error loss functions perform equally well for shifts of 15.0 to 30.0. For $m=100$, the modified squared error loss function again demonstrates consistent superiority across all shift sizes. As with the previous tables, the AEQL and PCI values underscore the effectiveness of the Bayesian method under the modified squared error loss function for $m=20$ and $m=100$, while the K loss function shows the best performance for $m=40$, achieving the lowest AEQL and a PCI of 1.

Table 5. Comparison of ARL and SDRL Values for Various Methods at $(\nu,\gamma)=(1,8)$

m	δ	Classical		SE_LF		MSE_LF		K_LF	
		ARL	SDRL	ARL	SDRL	ARL	SDRL	ARL	SDRL
20		L=3.0322		L=4.95054		L=4.97		L=4.95564	
	0.0	371.8129	371.3125	371.8815	371.3812	370.5558	370.0555	371.8571	371.3568
	0.1	354.7813	354.2810	343.5037	343.0033	342.1531	341.6527	343.4835	342.9832
	0.5	292.1143	291.6138	255.2386	254.7381	254.5723	254.0718	255.2204	254.7199
	1.0	221.8204	221.3198	178.2614	177.7607	177.7977	177.2970	178.2526	177.7519
	2.0	122.3022	121.8012	91.97409	91.47272	91.68299	91.18161	91.96828	91.46691
	3.0	68.0108	67.5089	51.1755	50.6730	51.04864	50.5461	51.1717	50.6692
	5.0	24.1745	23.6692	19.0400	18.5333	19.0051	18.4984	19.0389	18.5322
	10.0	4.2553	3.7219	3.7165	3.1774	3.7127	3.1736	3.7162	3.1771
	15.0	1.7551	1.1512	1.6420	1.0267	1.6411	1.0258	1.6419	1.0267
	20.0	1.1955	0.4835	1.1637	0.4364	1.1634	0.4361	1.1636	0.4364
	30.0	1.0084	0.0923	1.0064	0.0806	1.0064	0.0805	1.0064	0.0806
AEQL		382.7503		332.9384		332.5270		332.9210	
PCI		1.1510		1.0012		1.0000		1.0012	
40		L=3.0335		L=4.048		L=4.0629		L=4.05159	
	0.0	372.2031	371.7027	372.0345	371.5342	372.0346	371.5343	372.0345	371.5342
	0.1	353.9042	353.4039	344.5434	344.0431	344.5435	344.0431	344.5434	344.0431
	0.5	280.4963	279.9959	256.0342	255.5337	256.0342	255.5337	256.0342	255.5337
	1.0	206.8516	206.3510	180.146	179.6453	180.146	179.6453	180.146	179.6453
	2.0	110.6492	110.1480	93.4163	92.9150	93.4163	92.9150	93.4163	92.9150
	3.0	61.4701	60.9680	52.0896	51.5871	52.0896	51.5871	52.0896	51.5871
	5.0	22.3895	21.8837	19.4722	18.9656	19.4722	18.9656	19.4722	18.9656
	10.0	4.1101	3.5753	3.7952	3.2570	3.7952	3.2570	3.7952	3.2570
	15.0	1.7338	1.1279	1.6649	1.0521	1.6649	1.0521	1.6649	1.0521
	20.0	1.1890	0.4741	1.1699	0.4458	1.1699	0.4458	1.1699	0.4458
	30.0	1.0078	0.0891	1.0067	0.0822	1.0067	0.0822	1.0067	0.0822
AEQL		365.4377		336.8172		336.8172		336.8172	
PCI		1.0850		1.0000		1.0000		1.0000	
100		L=3.03492		L=3.4491		L=3.454		L=3.45	
	0.0	370.2639	369.7636	370.6674	370.1671	370.7171	370.2168	370.6270	370.1266
	0.1	348.2213	347.7209	343.8273	343.327	343.8337	343.3333	343.7625	343.2622
	0.5	270.3785	269.8781	256.4417	255.9412	256.4119	255.9115	256.384	255.8835
	1.0	195.8382	195.3375	180.6034	180.1027	180.5951	180.0944	180.5866	180.0859
	2.0	103.9681	103.4669	94.4945	93.9932	94.4827	93.9813	94.4817	93.9804
	3.0	57.9541	57.4519	52.7383	52.2359	52.7310	52.2286	52.7309	52.2285
	5.0	21.3939	20.8879	19.7780	19.2717	19.7758	19.2693	19.7758	19.2693
	10.0	4.0404	3.5049	3.8600	3.3226	3.8597	3.3223	3.8597	3.3223
	15.0	1.7214	1.1144	1.6813	1.0703	1.6812	1.0702	1.6812	1.0702
	20.0	1.1853	0.4687	1.1739	0.4519	1.1739	0.4518	1.1739	0.4518
	30.0	1.0075	0.0872	1.0069	0.0832	1.0068	0.0832	1.0068	0.0832
AEQL		355.5861		339.5716		339.5419		339.5400	
PCI		1.0473		1.0001		1.0000		1.0000	

Table 5 presents the results for hyper-parameters $(\nu,\gamma)=(1,8)$. For an inspection unit size of $m=20$, the Bayesian method under the modified squared error loss function outperforms the others across all magnitudes of mean shifts, yielding the lowest ARL_1 and $SDRL_1$ values. For $m=40$, all three Bayesian loss functions perform equally well, producing the same low ARL_1 and $SDRL_1$ values. In the case of $m=100$, the K loss function provides better detection for small shifts (0.1 to 3.0), while both the modified squared error and K loss functions perform comparably for larger shifts (5.0 to 30.0).

Consistent with previous tables, the AEQL and PCI values highlight the superior performance of the Bayesian approach. Specifically, for $m=20$, the modified squared error loss function yields the lowest AEQL and a PCI of 1. For $m=40$, all three Bayesian loss functions achieve the same result. Meanwhile, for $m=100$, the K loss function demonstrates the best performance, attaining the lowest AEQL and a PCI of 1.

Application to Real Dataset

This section provides a comparative analysis of the performance of classical and Bayesian c-charts, developed using the original squared error, modified squared error, and K loss functions. The demonstration is based on a real-world dataset involving the inspection of missing rivets on large aircraft. Specifically, 26 consecutive samples were collected, each representing the count of missing rivets per aircraft. It is assumed that the number of nonconformities in each sample follows a Poisson distribution, consistent with the assumption that the defects occur randomly and independently across the aircraft structure [5].

This dataset serves as a practical case study for assessing the effectiveness of each control chart method in detecting shifts in the process mean. The Poisson mean parameter was estimated using both the classical (frequentist) method and three Bayesian approaches based on the respective loss functions. These estimates were then used to construct control limits for monitoring shifts in the mean number of defects. For all Bayesian charts, the control width was set using a constant $L=3$, and the hyperparameters were specified as $(\nu,\gamma)=(1,8)$. The comparative performance of the four control charting approaches is illustrated in Figures 1 through 4.

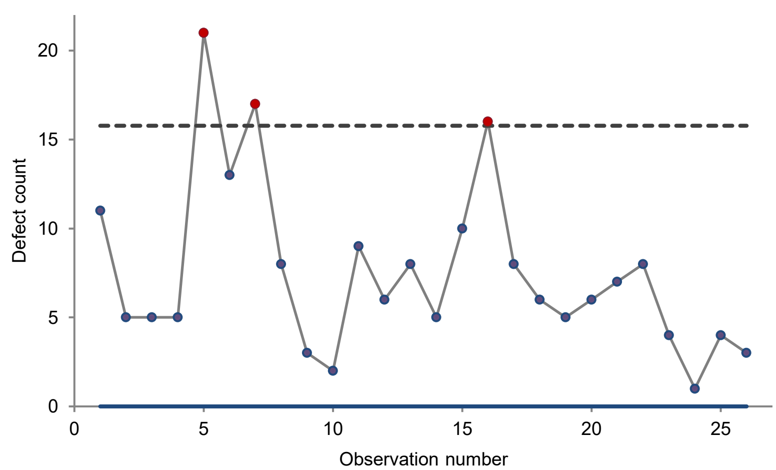

Figure 1. Classical c-chart for monitoring missing rivet counts in aircraft inspection data, illustrating baseline detection performance

Figure 1 displays the classical c-chart applied to the observed data. The chart signals out-of-control conditions at the 5th, 7th, and 16th observations. However, the chart detects these shifts only after several observations, indicating delayed signaling and lower sensitivity to early or subtle changes in the process mean. This limitation emphasizes the potential value of more adaptive techniques, such as Bayesian methods, in quality-sensitive industrial applications.

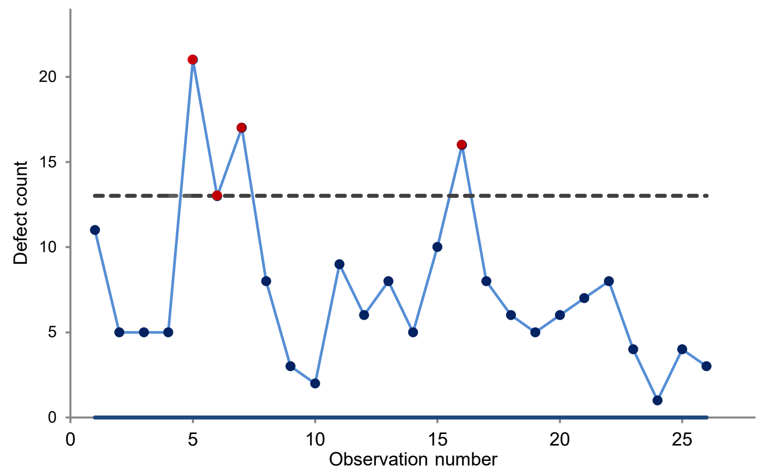

Figure 2. Bayesian c-chart based on the original squared error loss function for monitoring missing rivet counts, demonstrating improved sensitivity and earlier detection compared to the classical c-chart

Figure 2 shows the performance of the Bayesian c-chart constructed using the original squared error loss function. This chart detects out-of-control signals earlier, beginning at the 5th observation and continuing through the 7th, 16th, and 27th samples. The earlier identification of process anomalies demonstrates the improved sensitivity of this Bayesian method, offering practical advantages in industrial settings where early detection can help minimize defects, reduce waste, and maintain consistent product quality.

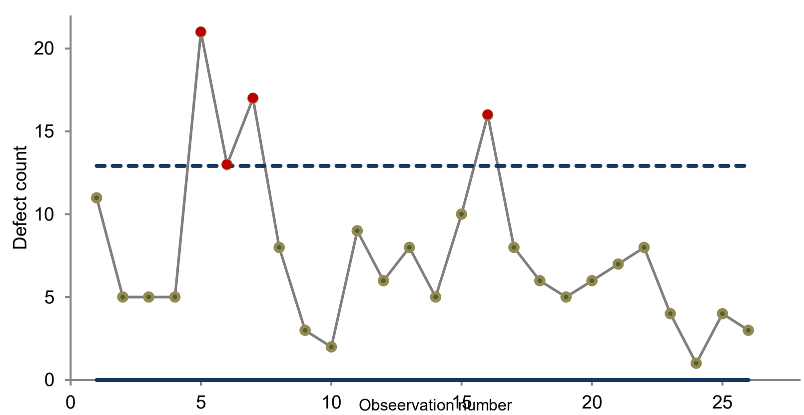

Figure 3. Bayesian c-chart based on the modified squared error loss function for monitoring missing rivet counts, highlighting enhanced early detection of process mean shifts

Figure 3 illustrates the results using the modified squared error loss function. Similar to the previous Bayesian approach, this method detects nonconforming observations at the 5th through 7th, 16th, and 27th inspection points. These results confirm that the modified squared error loss function enhances early detection capability, enabling quicker identification of mean shifts than the classical method.

Figure 4 presents the results for the Bayesian c-chart constructed using the K loss function. This chart also signals at the 5th through 7th, 16th, and 27th observations, demonstrating consistent and rapid detection performance comparable to the other Bayesian charts. The similarity of results across different loss functions highlights the robustness of the Bayesian framework in real-world applications.

Overall, the real-data application clearly demonstrates that Bayesian c-charts detect process shifts more quickly and consistently than the classical c-chart. All three Bayesian approaches identify out-of-control conditions at earlier stages, indicating higher sensitivity to mean shifts and stronger practical effectiveness. These findings confirm the suitability of Bayesian control charts for early detection and proactive quality control in industrial environments.

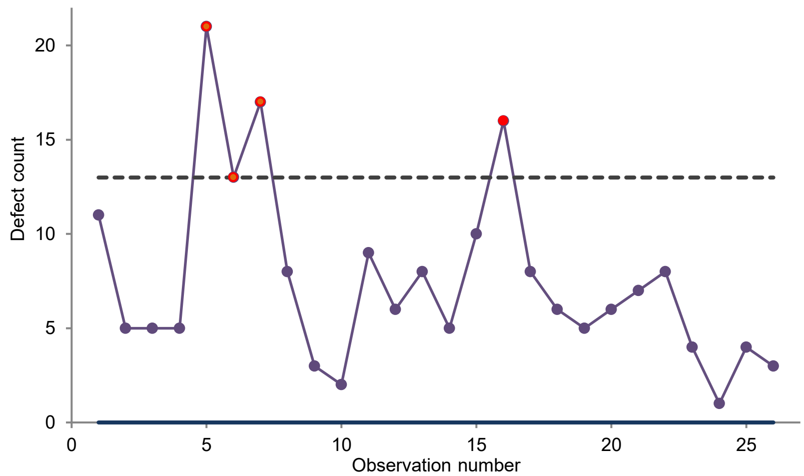

Figure 4. Bayesian c-chart constructed using the K loss function for monitoring missing rivet counts, showing detection performance comparable to other Bayesian approaches

The psychological impact of using control charts should not be underestimated. By providing clear and timely visual feedback, these charts support rapid decision-making and promote a culture of continuous improvement among quality personnel. The dataset analyzed here forms part of a broader investigation that reported substantial improvements, underscoring the value of control charts as essential tools for effective process monitoring and quality enhancement.

Conclusion and Discussion

This study proposes two enhanced Bayesian control chart methods—the modified squared error loss function and the K loss function—to improve the performance of the traditional c-chart in detecting process shifts. Through extensive simulation studies under various scenarios of shift magnitudes, inspection unit sizes (m = 20, 40, 100), and hyper-parameter settings, the results confirm that these Bayesian approaches outperform the classical method across multiple performance metrics.

In particular, the Bayesian method under the modified squared error loss function consistently demonstrated the lowest Average Run Length (ARL_1), Standard Deviation of Run Length ($SDRL_1$), Average Expected Quadratic Loss (AEQL), and Performance Comparison Index (PCI) across most scenarios. The K loss function also provided strong performance, especially in detecting small to moderate shifts, offering comparable or superior detection capability in certain cases.

The application to real-world data involving missing rivets in aircraft further confirms the effectiveness of the proposed methods. Both the modified squared error and K loss function-based Bayesian c-charts were able to detect out-of-control points earlier than the classical c-chart. This early detection is critical in industrial settings, where delays in identifying quality issues can lead to increased defects, costs, and safety risks.

The findings suggest that incorporating loss functions into Bayesian control charts allows for more flexible and sensitive monitoring systems that can be adapted to specific operational goals or risk tolerances. Moreover, the proposed methods show practical value in real-world process control environments, particularly those requiring high responsiveness and precision.

In conclusion, the modified squared error and K loss functions introduced in this study offer valuable extensions to the Bayesian c-chart framework. These approaches significantly improve the ability to detect process shifts over classical methods, making them suitable alternatives for modern quality control applications. Future work could explore their integration into dynamic systems with real-time updating, multivariate extensions, or applications in digital manufacturing environments.

Conflicts of Interest

The authors declare that there is no conflict of interest regarding the publication of this paper.

Acknowledgment

The author declares that there is no funding or institutional support to acknowledge.

References

[1] Mbaye, M. F., Sarr, N., & Ngom, B. (2021). Construction of control charts for monitoring various parameters related to the management of the COVID-19 pandemic. Journal of Biosciences and Medicines, *9*, 9–19.
[2] Mei, M. Q., Wang, L., & Yan, J. (2023). Maintaining product quality consistency when offshoring to emerging markets: The role of subsidiary control. *Journal of International Management, 29(1)*, 100989.
[3] Espinoza, J. L. V., Delgado, F. M. C., Rodriguez, V. H. P., Galvez, C. V. C., Lingan, R. Y. C., Ramírez, F. B., & Huaman, E. T. (2023). Product quality and customer loyalty: The case of a chocolate production cooperative, Peru. *Journal of Law and Sustainable Development, 11(7)*, e490.
[4] Costa Junior, A. M. da, Barros, J. G. M. de, Almeida, M. da G. D., Carvalho, C. P. de, & Sampaio, N. A. de S. (2023). Application of the Poisson distribution in the prediction of the number of defects in a textile factory. *Management and Administrative Professional Review, 14(8)*, 14378–14386.
[5] Burr, J. T. (2004). *Element Statically Quality Control*. Taylor & Francis Group, LLC, New York, USA.
[6] Montgomery, D. C. (2009). *Introduction to Statistical Quality Control*. John Wiley & Sons, Inc, New York, USA.
[7] Supharakonsakun, Y. (2024). Bayesian control chart for number of defects in production quality control. *Mathematics, 12(12)*, 1903.
[8] Bayarri, M. J., & Garcia-Donato, G. (2005). A Bayesian sequential look at u-control charts. *Technometrics, 47(2)*, 142–151.
[9] Calabrese, J. M. (1995). Bayesian process control for attributes. *Management Science, 41(4)*, 637–645.
[10] Taylor, H. M. (1965). A Markov quality control process subject to partial observation. *ANNALS OF Mathematical Statistics, 36(5)*, 1677–1694.
[11] Taylor, H. M. (1969). Statistical control of a Gaussian process. *Technometrics, 9(1)*, 29–41.
[12] Saghir, A., Lin, Z., Chen, C.-W., & Lu, Z. (2015). The properties of the geometric Poisson exponentially weighted moving control chart with estimated parameters. *Cogent Mathematics, 2(1)*, 992381.
[13] Menzefricke, U. (2013). Combined exponentially weighted moving average charts for the mean and variance based on the predictive distribution. *Communications in Statistics – Theory and Methods, 42(22)*, 4003–4016.
[14] Menzefricke, U. (2013b). Control charts for the mean and variance based on changepoint methodology. *Communications in Statistics – Theory and Methods, 42(6)*, 988–1007.
[15] Riaz, S., Riaz, M., Hussain, Z., & Abbas, T. (2017). Monitoring the performance of Bayesian EWMA control chart using loss functions. *Computers & Industrial Engineering, 112*, 426–436.
[16] Aslam, M., & Anwar, S. M. (2020). An improved Bayesian Modified-EWMA location chart and its applications in mechanical and sport industry. *PLOS ONE, 15(2)*, e0229422.
[17] Huberts, L. C. E., Goedhart, R., & Does, R. J. M. M. (2022). Improved control chart performance using cautious parameter learning. *Computers & Industrial Engineering, 169*, 108185.
[18] Javed, A., Abbas, T., & Abbas, N. (2024). Developing Bayesian EWMA chart for change detection in the shape parameter of inverse Gaussian process. *PLOS ONE, 19(5)*, e0301259.
[19] Abbas, T., Javed, A., & Abbas, B. (2024). Bayesian enhanced EWMA scheme for shape parameter surveillance in inverse Gaussian models. *Computers & Industrial Engineering, 197*, 110637.
[20] Ali, S. (2020). A predictive Bayesian approach to EWMA and CUSUM charts for time-between-events monitoring. *Journal of Statistical Computation and Simulation, 90(16)*, 3025–3050.
[21] Assareh, H., Noorossana, R., & Mengersen, K. (2013). Bayesian change point estimation in Poisson-based control charts. *Journal of Industrial Engineering International, 9(1)*, 1–9.
[22] Raubenheimer, L., & van der Merwe, A. (2015). Bayesian control chart for nonconformities. *Quality and Reliability Engineering International, 31(8)*, 1359–1366.
[23] Supharakonsakun, Y. (2024). Empirical Bayes prediction for an attribute control chart in quality monitoring. *IEEE Access, 12*, 160784–160793.
[24] Mitchell, C., Abdel-Salam, A. S., & Mays, D. A. (2020). Bayesian EWMA and CUSUM control charts under different loss functions. *arXiv Preprint*, arXiv:2009.09844.
[25] Chakraborti, S., & Human, S. W. (2008). Properties and performance of the c-chart for attributes data. *Journal of Applied Statistics, 35(1)*, 89–100.
[26] Song, J. J., & Kim, J. (2017). Bayesian estimation of rare sensitive attribute. *Communications in Statistics – Simulation and Computation, 46(5)*, 4154–4160.
[27] Wald, A. (1939). Contributions to the theory of statistical estimation and testing hypotheses. *Annals of Mathematical Statistics, 10(4)*, 299–326.
[28] Noor-ul-Amin, M., & Noor, S. (2021). An adaptive EWMA control chart for monitoring the process mean in Bayesian theory under different loss functions. *Quality and Reliability Engineering International, 37(2)*, 804–819.

[29] Abdullah, H., & Aref, R. (2016). Bayesian inference for parameter and reliability function of inverse Rayleigh distribution under modified squared error loss function. *Australian Journal of Basic and Applied Sciences, 10(16)*, 241–248.

[30] Jabeen, R., & Zaka, A. (2021). The modified control charts for monitoring the shape parameter of weighted power function distribution under classical estimator. *Quality and Reliability Engineering International, 37(8)*, 3417–3430.

[31] Tinochai, K., & Jampachaisri, K. (2022). The performance of empirical Bayes based on weighted squared error loss and K-loss functions in skip lot sampling plan with resampling. *Engineering Letters, 30(2)*, 770–781.

[32] Zhang, Y.-Y. (2020). The Bayesian posterior estimators under six loss functions for unrestricted and restricted parameter spaces. *IntechOpen*.

[33] Supharakonsakun, Y. (2025). Performance enhancement of c-chart via Bayesian method. *Engineering Letters, 33(12)*, 4859–4871.